Origin of structures in the low-energy single-electron continuum in calculations for ion collisions from argon

L. Gulyás,[1,2] T. Kirchner,[3] T. Shirai,[1] and M. Horbatsch[3]
[1]*Japan Atomic Energy Research Institute Tokai-mura, Ibaraki, 319-1195, Japan*
[2]*Institute of Nuclear Research of the Hungarian Academy of Sciences (ATOMKI), P.O. Box 51, H-4001 Debrecen, Hungary*
[3]*Department of Physics and Astronomy, York University, Toronto, Ontario, Canada M3J 1P3*
(Received 16 March 2000; revised manuscript received 25 April 2000; published 5 July 2000)

Doubly differential cross sections for inclusive single-electron emission in 3.6 MeV/amu Au^{53+} + Ar collisions are calculated in the *continuum distorted wave with eikonal initial-state* approximation. Previously observed structures in the low-energy continuum are traced back to a known deficiency of the Hartree-Fock-Slater target potential that has been used in the work [R. Moshammer *et al.*, Phys. Rev. Lett. **83**, 4721 (1999)]. The structures do not occur, if the argon atom is described in terms of the *optimized potential method*, in which the electronic exchange interaction is treated exactly.

PACS number(s): 34.50.Fa

I. INTRODUCTION

Recent experimental and theoretical studies in the field of fast ion-atom collisions have been concerned with the question whether signatures of the initial-state momentum distribution of the electronic target system are mapped to electron-emission spectra in a direct fashion. This issue has been discussed extensively in double ionization of helium [1], where several kinematically complete experiments with different projectile charges and velocities have been performed [2]. Calculations in the Born approximation with shake-off have led to the conclusion that the momentum distributions of the emitted electrons are sensitive to the specific initial-state wave function [3]. It was also found that the spectra vary with the model used for the description of the final state, and that it is difficult to disentangle the effects of the initial and final states on the cross sections.

A recent joint experimental and theoretical study focused on low-energy single-electron emission spectra obtained from 3.6 MeV/amu Au^{53+} impact on neon and argon atoms [4]. The calculations relied on an effective single-particle description of the collision process, and were performed in the *continuum distorted wave with eikonal initial-state* (CDW-EIS) approximation introduced by Crothers and McCann [5]. In the specific model used, the undisturbed bound and continuum eigenstates were obtained by solving the stationary Schrödinger equation with Hartree-Fock-Slater (HFS) model potentials for the target atoms.

The theoretical results reported in Ref. [4] were in good agreement with experimental doubly differential cross sections (DDCS) obtained from a summation of measured one-, two-, and three-electron ionization events according to the degree of ionization. The summation is necessary, since the calculated single-electron emission spectra correspond to *inclusive* processes [6] where the final state of one electron is specified, while nothing is known about the final states of the other electrons. We note that the term inclusive single ionization is equivalent to the term net ionization that we have used previously [7]. In the case of argon targets, the CDW-EIS results of Ref. [4] showed a shoulder as a function of the longitudinal electron velocity $v_\parallel$ for the lowest transverse velocity cut $v_\perp = 0.05$ a.u. This structure was qualitatively supported by the experimental data and was attributed to the nodal structure of the momentum distribution of the initial argon $3p_0$ orbital, which contributes dominantly to the DDCS in this region.

It is the purpose of the present paper to show that this interpretation is not correct. We have repeated the CDW-EIS calculation with the HFS potential and in addition have performed a calculation with a more accurate target potential obtained from the *optimized potential method* (OPM) [8]. We demonstrate that the shoulder in the theoretical results is an artifact, which is caused by a known deficiency of the HFS potential. It is introduced into the low-energy DDCS via the final single-particle states and cannot be related to the initial states. Moreover, it does not occur if the OPM potential is used in the calculation. Structures, which might reflect the momentum distributions of the initial orbitals, are found in the theoretical DDCS in other regions, but are not supported by the experimental data of Ref. [4].

II. THEORETICAL ASPECTS

The effective single-particle representation of the target atom can be based on the Kohn-Sham scheme of density-functional theory (DFT) [9]. In this scheme the atomic potential is usually split according to ($\hbar = m_e = e = 1$)

$$v_{\rm atom}(r) = -\frac{Q_T}{r} + \int \frac{n(r')}{|\mathbf{r}-\mathbf{r}'|} d^3r' + v_{xc}([n],r), \qquad (1)$$

where Q_T denotes the nuclear charge and $n(r')$ is the one-particle density of the electronic system. The exchange-correlation potential v_{xc} is a functional of n and has to be approximated in any practical scheme.

In the HFS approximation, the exchange part v_x is given by the average exchange-interaction energy of a single electron in a homogeneous electron gas. As $v_x^{\rm HFS}$ decreases ex-

ponentially in the asymptotic region, the correct $-1/r$ tail is introduced *a posteriori* via the so-called Latter correction [10]

$$v_x^{\mathrm{HFS/L}}(r)=\begin{cases} v_x^{\mathrm{HFS}}(r) & \text{for} \quad v_x^{\mathrm{HFS}}(r)<-1/r \\ -1/r & \text{elsewhere.} \end{cases} \tag{2}$$

Since the Latter correction is used throughout the present work, we will identify the HFS/L model with HFS in the following.

In contrast to this approximate treatment of electronic-exchange effects, the OPM provides the exact exchange-only limit of the exchange-correlation functional. The potential used in the present calculation furthermore includes a correlation contribution in the approximation of Colle and Salvetti [11]. This contribution improves the ground-state energy of the system, but for the noble gases the corresponding potential v_c has an incorrect sign in the valence region [12]. Previous studies for ionization and electron capture from neon atoms showed that cross sections obtained from an OPM description of the target were reproduced if the Colle-Salvetti correlation contribution was turned off [7], simply because the magnitude of v_c is too small to affect the results. Considering these earlier findings, we conjecture that v_c is also of minor importance for the present analysis.

In the CDW-EIS approximation of ionization, transition amplitudes are calculated in first order of a perturbative series

$$a_{if}=-i\int_{-\infty}^{+\infty} dt\langle \chi_f^-|(\hat{h}-i\partial_t)|\chi_i^+\rangle \tag{3}$$

with the single-particle Hamiltonian

$$\hat{h}=-\frac{1}{2}\Delta+v_{\mathrm{atom}}(r)-\frac{Q_P}{|\mathbf{r}-\mathbf{R}|}, \tag{4}$$

where Q_P and $\mathbf{R}$ denote the charge and coordinate of the projectile, respectively. The initial states χ_i^+ and final states χ_f^- are taken to be products of undisturbed target orbitals and specific distortion factors, which account for the Coulomb interaction with the projectile and ensure that the boundary conditions of the collision problem are satisfied. As in Ref. [4], we have solved the stationary Schrödinger equation with the HFS and OPM potentials to obtain the undisturbed bound and continuum eigenfunctions of the target atom. This procedure guarantees the orthogonality between initial and final states. It was shown to improve upon previous versions of the CDW-EIS approximation where the initial and final states were chosen as eigenfunctions of different single-particle Hamiltonians (for details of the method see Ref. [13]).

III. DISCUSSION

We start the discussion with a comparison of the initial-state momentum distributions as obtained from the OPM and HFS descriptions of argon. Figure 1 shows the radial probability distributions of the (undisturbed) $3s$ and $3p$ orbitals,

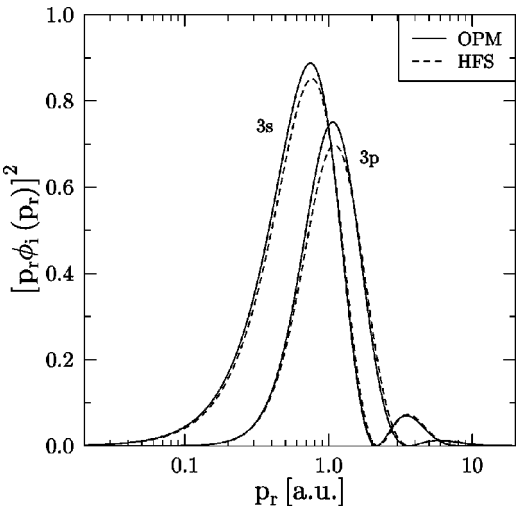

FIG. 1. Radial probability density of the $3s$ and $3p$ orbitals in atomic units obtained from the OPM and HFS descriptions of the argon ground state as a function of the radial momentum.

which are dominantly ionized in the collision process considered. The OPM and HFS eigenfunctions are very similar in both cases. The first maxima of the OPM orbitals lie slightly above the HFS values, but the positions of all maxima and nodes coincide almost exactly (note that the $3s$ orbital has a second node at radial momentum $p_r\approx 8.5$ a.u. and a very weak third maximum at $p_r\approx 13$ a.u.).

Despite the strong similarities of the initial states, the DDCS obtained from the OPM and HFS descriptions show some striking differences. Following Ref. [4], we present the DDCS in cylindrical coordinates in velocity space in Fig. 2. For the lowest transverse velocity cut $v_\perp=0.05$ a.u., the HFS results show the shoulder at $v_\parallel\approx 0.5$ a.u. that was discussed in Ref. [4]. By contrast, when the OPM is used in the CDW-EIS calculation, the DDCS falls off smoothly as a function of the longitudinal velocity. As this different behavior occurs while very similar initial-state wave functions are used, we conclude that the origin of the shoulder in the case of HFS is not related to the $3p$ momentum distribution.

As a general trend in all transverse velocity cuts the DDCS's obtained from the OPM description are smaller than the corresponding HFS data. This leads to a total cross section, which is about 25% smaller than the HFS result. This observation agrees with the results of a recent analysis of total cross sections in $p+\mathrm{Ar}$ collisions [14], and can be understood from the different binding properties of the initial states; e.g., one finds the $3p$ energy eigenvalue to equal -0.620 a.u. in the case of OPM, and -0.533 a.u. in the case of HFS. The OPM orbitals are more tightly bound and thus less likely to be ionized.

In addition to the theoretical results, we have also included the experimental DDCS of Ref. [4] summed over the degree of ionization in Fig. 2. In Ref. [4] they were normalized to the theoretical HFS model based calculations. We have normalized the experimental DDCS to the present results based on the OPM potential, which amounts to a reduction by a factor of 0.75. The agreement between the theoretical and experimental DDCS is very convincing when the CDW-EIS calculations are performed with the OPM poten-

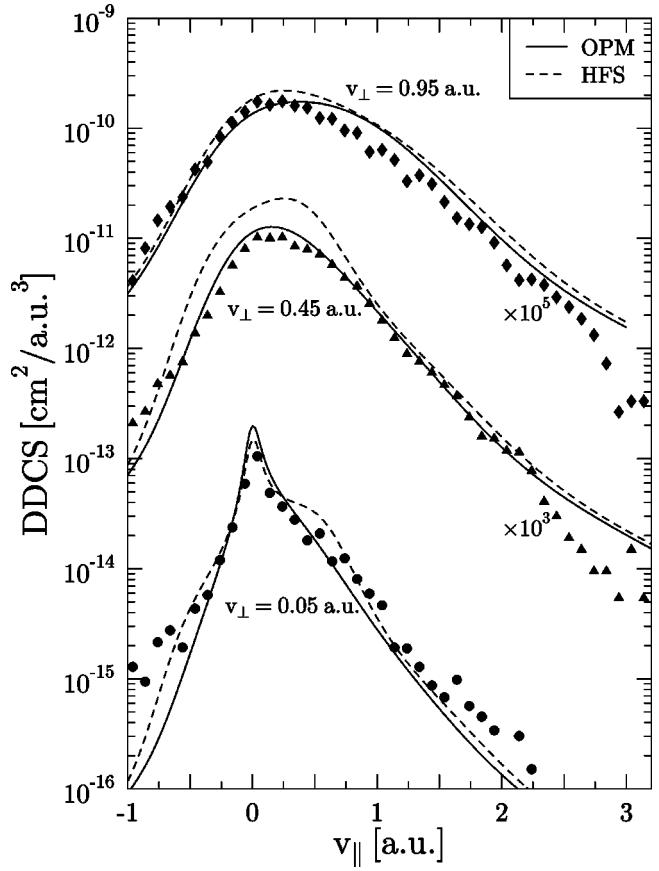

FIG. 2. Doubly differential cross section, $d^2\sigma/(dv_\parallel dv_\perp 2\pi v_\perp)$, for inclusive single-electron emission in 3.6 MeV/amu Au^{53+} + Ar collisions. The DDCS is shown as a function of the longitudinal electron velocity $v_\parallel$ for certain transverse velocity ($v_\perp$) cuts. The DDCS at $v_\perp = 0.45$ and 0.95 a.u. are multiplied by the indicated factors. Symbols: experimental data from Ref. [4] normalized to the present results of the CDW-EIS calculation with the OPM potential.

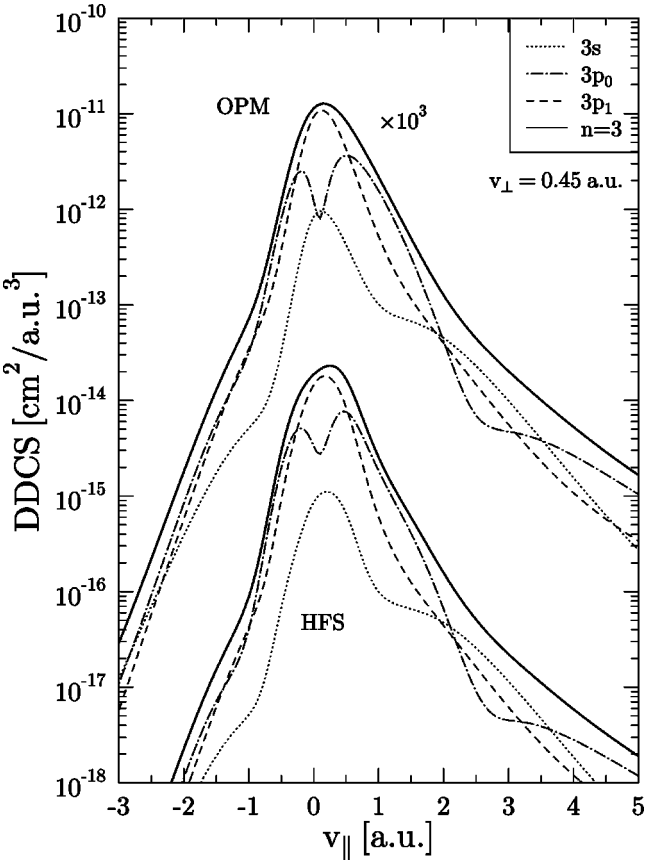

FIG. 3. Individual contributions of the $3s$ and $3p$ initial states to the DDCS at $v_\perp = 0.45$ a.u. as a function of $v_\parallel$. The OPM results are multiplied by the indicated factor.

tial. Only at large longitudinal-electron velocities do the experimental results fall off more steeply in the forward direction and more flatly in the backward direction than the theoretical data. The DDCS obtained from the HFS description of the argon atom exhibits additional discrepancies for the transverse velocity cut at $v_\perp = 0.45$ a.u.. We note that these discrepancies are also observed in Fig. 3 of Ref. [4] and are not a consequence of the normalization of the experimental data to the present results based on the OPM potential.

In Fig. 3 we show the individual contributions of the $3s$ and $3p$ initial states to the DDCS at $v_\perp = 0.45$ a.u.. These contributions are weighted according to the numbers of electrons available in the orbitals. Remarkably, for both the OPM and HFS approximations they show structures that might reflect the initial-state momentum distributions in a qualitative fashion. For example, the contribution from the $3s$ initial state has a shoulder at $v_\parallel \approx 2$ a.u.. This might be related to the second peak in the initial-state momentum distribution (cf. Fig. 1), which corresponds to electrons that are rather close to the target nucleus in position space. A similar observation is made for the $3p_0$ initial state, which is aligned along the ion-beam axis. In addition, this contribution exhibits a minimum at $v_\parallel = 0$ a.u., indicating a suppression of ionization perpendicular to the orientation of the initial state. By contrast, the perpendicularly aligned $3p_1$ orbital gives rise to a maximum at $v_\parallel = 0$ a.u. and a rather narrow distribution as a function of the longitudinal electron velocity $v_\parallel$.

However, these distinct structures of the individual contributions cannot be found in the experimental DDCS presented in Fig. 2. The shoulders of the $3s$ and $3p_0$ initial states at large $v_\parallel$ are in contradiction to the steep decrease of the experimental DDCS in this region, while the minimum in the $3p_0$ contribution at $v_\parallel = 0$ a.u. is masked by the contributions of the other initial states to the DDCS.

We now turn to the analysis of the different behavior in the DDCS at $v_\perp = 0.05$ a.u., which occurs when the OPM and HFS atomic potentials are used, respectively. The individual contributions of the $3s$ and $3p$ initial states to this DDCS are shown in Fig. 4. We restrict the discussion to relatively small longitudinal electron velocities $v_\parallel$, but note that in analogy to the case of $v_\perp = 0.45$ a.u., structures are observed at larger $v_\parallel$. For both OPM and HFS descriptions, the $3p_0$ state gives the dominant contribution to the DDCS particularly at intermediate longitudinal velocities, even though it is occupied by two electrons only as compared to four electrons in the $3p_1$ state. The details of the individual distributions are quite different for the calculations based on the OPM and HFS atomic potentials, respectively. In the

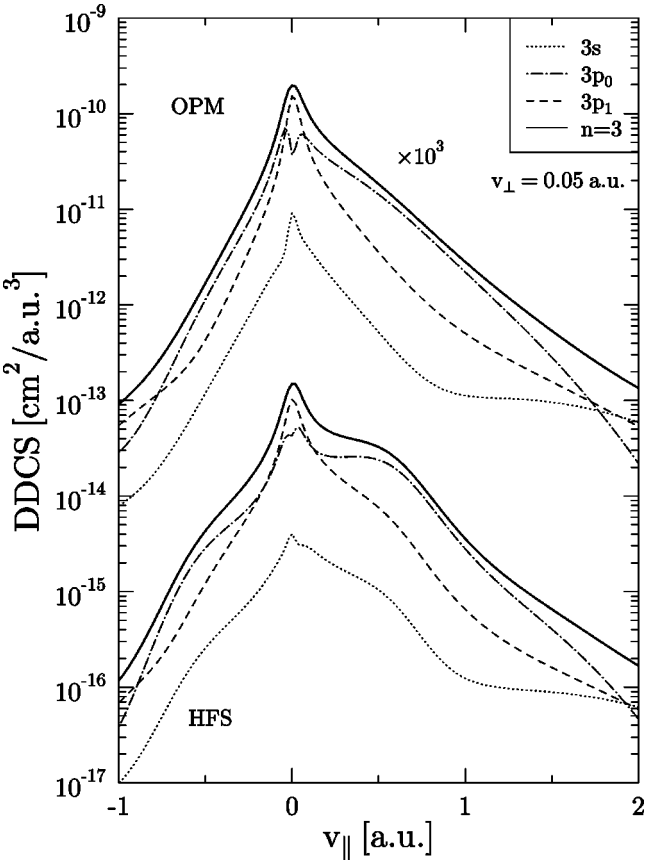

FIG. 4. Individual contributions of the $3s$ and $3p$ initial states to the DDCS at $v_\perp = 0.05$ a.u. as a function of $v_\parallel$. The OPM results are multiplied by the indicated factor.

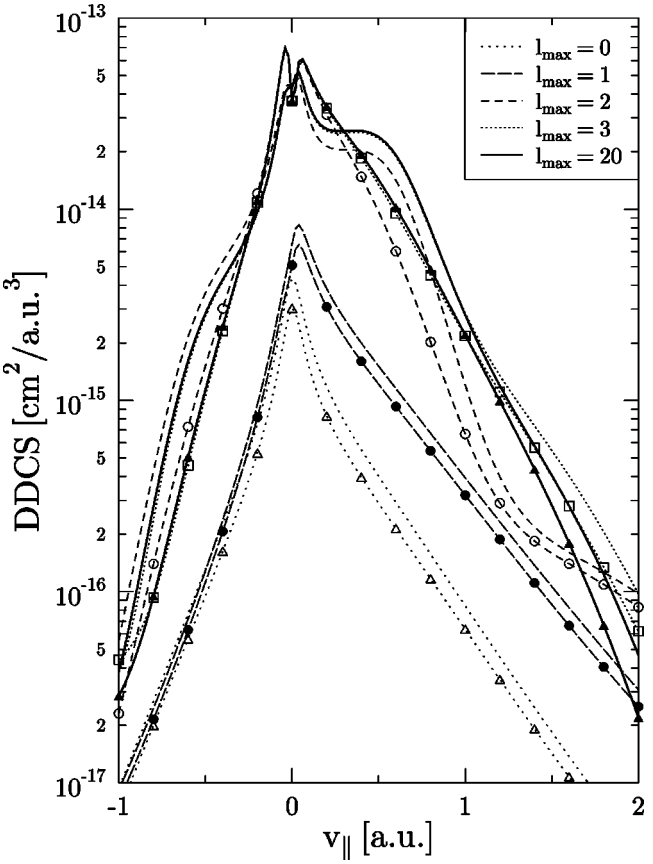

FIG. 5. DDCS at $v_\perp = 0.05$ a.u. for the $3p_0$ initial-state and partial-wave expansions restricted to $l_{\max} = 1,2,3,20$ as a function of $v_\parallel$. Lines, results obtained from the HFS approximation; lines with symbols, results obtained from the OPM.

latter case the shoulder in the total DDCS at $v_\parallel \approx 0.5$ a.u. is mainly caused by the $3p_0$ electrons, but similar structures are also observed in the $3p_1$ and $3s$ contributions. By contrast, all OPM orbitals give rise to smooth curves. The suppression of ionization perpendicular to the orientation of the initial $3p_0$ orbital is almost completely compensated by the divergence of the DDCS in the limit $v \to 0$ [4].

In addition to the results presented in Figs. 1 and 2, we have performed ''hybrid'' CDW-EIS calculations with HFS initial and OPM final states and vice versa. The results of these calculations have to be interpreted with some caution due to the inconsistent nature of the model. Nevertheless, they clearly indicate that the origin of the shoulder in the DDCS at $v_\perp = 0.05$ a.u. is not related to the initial but rather to the final states used in the calculation. For both HFS and OPM initial orbitals the shoulders occur for HFS final states and smooth curves are obtained in both cases for OPM final states.

The continuum eigenstates are implemented in a partial-wave expansion in the present CDW-EIS model. In order to illustrate the influence of the individual partial waves on the DDCS, we show results with restricted partial-wave expansions for $v_\perp = 0.05$ a.u. in Fig. 5. We focus on the $3p_0$ initial state but note that similar results have been observed for the other initial states as well. The distributions obtained from the OPM and the HFS descriptions are very similar if only $l=0$ or $l=0,1$ are considered. With the inclusion of the $l=2$ contribution, the shoulder occurs in the case of the HFS approximation, whereas the curve remains smooth in the case of the OPM. The higher partial waves give no qualitative changes, and the cross section is practically converged for $l_{max}=3$, except at high longitudinal velocities. The rapid convergence is due to the fact that the low-velocity cut corresponds to distant collisions, where transfer of one unit of angular momentum is most likely [7]. We have performed several further checks, which support the finding that the $l=2$ partial wave introduces the shoulder in the case of the HFS description. For example, we have repeated the calculations in the first Born approximation and we have studied the DDCS obtained from individual partial waves. We have also compared the OPM and HFS partial waves for low electron energies explicitly and have found striking differences for $l=2$.

The different behavior can be understood, if one considers the effective potentials

$$v_{\text{eff}}(r) = v_{\text{atom}}(r) + \frac{l(l+1)}{2r^2}, \tag{5}$$

for which the stationary Schrödinger equation is solved in order to generate the radial parts of the initial and final states. In Fig. 6 we show v_{eff} for $l=0,\ldots,3$ both for the OPM and

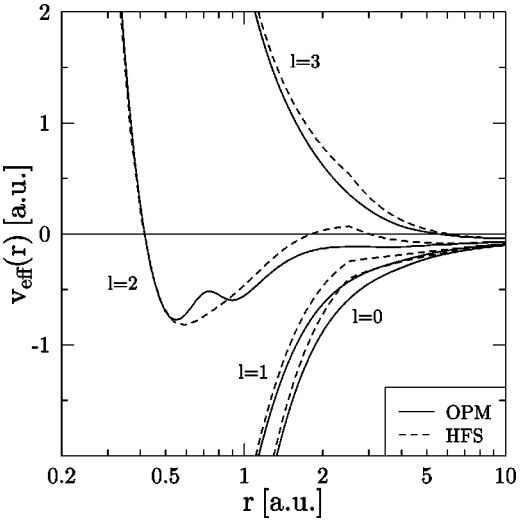

FIG. 6. Effective potentials [Eq. (5)] of neutral argon for $l=0,\ldots,3$.

the HFS approximations. One observes a slight kink in the HFS effective potentials, which is introduced by the sudden switching to the $-1/r$ behavior [cf. Eq. (2)]. For $l=2$, the competition between the atomic and the centrifugal potential shifts this kink into the region of the ionization threshold and produces a small potential barrier with a maximum height of 1.88 eV. It is evident that this barrier introduces errors in the eigenfunctions with $l=2$, in particular in the low-energy continuum states. By contrast, the OPM potential approaches the $-1/r$ tail smoothly. For $l=2$, one observes a structure around $r=0.8$ a.u., which is due to the exact exchange potential and reflects the shell structure of the atom [12].

IV. CONCLUSIONS

We conclude that the shoulder in the DDCS at $v_\perp=0.05$ a.u. obtained with the HFS description of argon is artificial and is not related to the nodal structure of the initial momentum distribution as was conjectured in Ref. [4]. We have found structures in the DDCS in other regions, which might reflect properties of the initial states, but they are not supported by the experimental data. We note that we have observed unphysical results with HFS target potentials in recent studies of other collision systems by means of the CDW-EIS approximation and the nonperturbative *basis generator method* [7,14], but have not provided a detailed explanation for the failure of the HFS description in that case. For low-energy electron emission in $Au^{53+}+Ar$ collisions, we have traced the occurrence of the shoulder back to the $l=2$ partial wave of the final continuum state. This partial wave gives the dominant contribution to the DDCS at low velocities (cf. Fig. 5), and is in error in the case of the HFS description as a consequence of the artificial barrier in the effective potential (Fig. 6).

We note that the authors of Ref. [4] also calculated DDCS for $Au^{53+}+Ne$ collisions with the CDW-EIS approximation and the HFS description of the target. In this case no shoulder was observed. If one inspects the corresponding effective potentials (5) for neon, one also notices the sudden switching to the $-1/r$ tail, but the competition with the centrifugal potential does not shift the kink into the threshold region. For $l=1$, the kink lies well below the ionization threshold, while it is in the repulsive region for $l=2$, where the centrifugal potential dominates. Therefore, one can expect that the Latter correction does not cause large errors in the continuum wave functions in this case.

In general, however, our study suggests to avoid HFS target potentials in calculations for ion-atom collisions, since the Latter correction can produce artificial structures in the low-energy continuum wave functions. When first-principles schemes like the OPM are not available, it might be a better choice to construct simple model potentials [15] than to use the HFS approximation.

ACKNOWLEDGMENTS

We thank E. Engel for making his OPM atomic structure calculations available to us. This work was partially supported by the Science and Technology Agency of Japan. T.K. would like to thank H. J. Lüdde for helpful discussions, and gratefully acknowledges the financial support of the DAAD.

[1] S. Keller, H. J. Lüdde, and R. M. Dreizler, Phys. Rev. A **55**, 4215 (1997); B. Bapat *et al.*, J. Phys. B **32**, 1859 (1999).
[2] R. Moshammer *et al.*, Phys. Rev. Lett. **77**, 1242 (1996); **79**, 3621 (1997).
[3] B. Bapat, S. Keller, R. Moshammer, and J. Ullrich, J. Phys. B **33**, 1437 (2000); S. Keller, B. Bapat, R. Moshammer, J. Ullrich, and R. M. Dreizler, *ibid.* **33**, 1447 (2000).
[4] R. Moshammer, P. D. Fainstein, M. Schulz, W. Schmitt, H. Kollmus, R. Mann, S. Hagmann, and J. Ullrich, Phys. Rev. Lett. **83**, 4721 (1999).
[5] D. S. F. Crothers and J. F. McCann, J. Phys. B **16**, 3229 (1983).
[6] H. J. Lüdde and R. M. Dreizler, J. Phys. B **18**, 107 (1985).
[7] T. Kirchner, L. Gulyás, H. J. Lüdde, E. Engel, and R. M. Dreizler, Phys. Rev. A **58**, 2063 (1998).
[8] E. Engel and S. H. Vosko, Phys. Rev. A **47**, 2800 (1993).
[9] R. M. Dreizler and E. K. U. Gross, *Density Functional Theory* (Springer, Berlin, 1990).
[10] R. Latter, Phys. Rev. **99**, 510 (1955).
[11] R. Colle and O. Salvetti, Theor. Chim. Acta **37**, 329 (1975).
[12] E. Engel and R. M. Dreizler, J. Comput. Chem. **20**, 31 (1999).
[13] L. Gulyás, P. D. Fainstein, and A. Salin, J. Phys. B **28**, 245 (1995).
[14] T. Kirchner, L. Gulyás, H. J. Lüdde, A. Henne, E. Engel, and R. M. Dreizler, Phys. Rev. Lett. **79**, 1658 (1997).
[15] A. E. S. Green, D. L. Sellin, and A. S. Zachor, Phys. Rev. **184**, 1 (1969); B. Hamre, J. P. Hansen, and L. Kocbach, J. Phys. B **32**, L127 (1999).